



Published in final edited form as:

Circ Res. 2015 February 27; 116(5): 797–803. doi:10.1161/CIRCRESAHA.116.305913.

RNA Sequencing of Mouse Sinoatrial Node Reveals an Upstream Regulatory Role for *Islet-1* in Cardiac Pacemaker Cells

Vasanth Vedantham^{1,2,6}, Giselle Galang^{1,2,6}, Melissa Evangelista^{1,6}, Rahul C. Deo^{2,4,5,6}, and Deepak Srivastava^{1,3,4}

¹Gladstone Institute of Cardiovascular Disease, San Francisco, CA

²Division of Cardiology, Department of Medicine, University of California, San Francisco, CA

³Department of Pediatrics, University of California, San Francisco, CA

⁴Department of Biochemistry and Biophysics, University of California, San Francisco, CA

⁵Institute for Human Genetics, California Institute for Quantitative Biosciences, University of California, San Francisco, CA

⁶Cardiovascular Research Institute, University of California, San Francisco, CA

Abstract

Rationale—Treatment of sinus node disease with regenerative or cell-based therapies will require a detailed understanding of gene regulatory networks in cardiac pacemaker cells (PCs).

Objective—To characterize the transcriptome of PCs using RNA sequencing, and to identify transcriptional networks responsible for PC gene expression.

Methods and Results—We used laser capture micro-dissection (LCM) on a sinus node reporter mouse line to isolate RNA from PCs for RNA sequencing (RNA-Seq). Differential expression and network analysis identified novel SAN-enriched genes, and predicted that the transcription factor *Islet-1* (*Isl1*) is active in developing pacemaker cells. RNA-Seq on SAN tissue lacking *Isl1* established that *Isl1* is an important transcriptional regulator within the developing SAN.

Conclusions—(1) The PC transcriptome diverges sharply from other cardiomyocytes; (2) *Isl1* is a positive transcriptional regulator of the PC gene expression program.

Keywords

Sinoatrial node; laser capture microdissection; *Isl1*; *Hcn4*; transcription factors; mouse heart development; RNA-Seq

Address correspondence to: Dr. Deepak Srivastava, Gladstone Institute of Cardiovascular Disease, 1650 Owens Street, San Francisco, CA 94158, TEL: 415-734-2716, FAX: 415-355-0141, dsrivastava@gladstone.ucsf.edu. Dr. Rahul C. Deo, Cardiovascular Research Institute, University of California, San Francisco, 555 Mission Bay Blvd South, Room 452S, San Francisco, CA, 94158, TEL: 415-476-9593, Rahul.Deo@ucsf.edu.

DISCLOSURES

None.

INTRODUCTION

Pacemaker cells (PCs) within the sinoatrial node (SAN) generate the electrical impulse that initiates each heartbeat. Sinus node dysfunction (SND), characterized by loss of PCs and SAN fibrosis, is a common but poorly understood disease. With the advent of cellular reprogramming technology,^{1, 2} there is increasing interest in understanding gene regulatory networks in PCs, both to improve our understanding of SND and to facilitate novel therapies such as biological pacemakers and SAN regeneration.

Transcription factors important for SAN development and function have been identified, including *Tbx18*,³ *Tbx3*,⁴ *Shox2*,⁵ and *Isl1*.^{6, 7} Efforts to reprogram non-PCs into PCs have employed some of these SAN transcription factors,^{8–10} even though their downstream transcriptional networks have not been fully elucidated.

Although these efforts are highly promising, there have been no genome-wide transcriptome comparisons of putatively reprogrammed PC-like cells with *bona fide* PCs, largely because of the absence of PC transcriptome data. Transcriptional profiling of PCs presents special challenges because of the lack of specific molecular markers, the small size of the developing SAN, and the interdigitation of PCs with non-PCs in the SAN. At present, the lack of transcriptome data from PCs remains a barrier to further progress in understanding SAN biology, and to assessing and improving the fidelity of PC reprogramming technology.

METHODS

Laser capture microdissection

Embryos or hearts were removed intact, washed with cold PBS, and immediately embedded in OCT and stored at -20°C until sectioning. Tissue was sectioned at a thickness of 8 microns onto membrane-coated slides (MembraneSlide NF 1.0 PEN, Zeiss Microscopy, Gottingen, Germany). For laser capture, slides were thawed to room temperature until evaporation of moisture (approximately 1 minute), placed on the microscope stage of a PALM Micro-Beam inverted microscope with LCM capability (Zeiss). The sinus node tissue was identified visually and outlined manually with the microscope user interface (Online Video II). Laser power and catapult energy were optimized prior to the experiment and varied from experiment-to-experiment. After each experiment, sections were stained with DAPI and anti-Hcn4, mounted, and visualized to confirm accurate dissection of the region of interest.

A detailed methods section is available online.

RESULTS

Laser capture micro-dissection of cardiac pacemaker cells for RNA sequencing

Hcn4-GFP BAC transgenic mice exhibited high-level GFP expression in the sinoatrial node (SAN) and venous pole at E12.5, with further restriction of expression to the SAN at P0 and in the adult heart (Figure 1A).¹¹ GFP expression was complementary to Connexin-40, a marker of working atrial myocytes, and isolated adult GFP⁺ cells showed morphology

typical of PCs and exhibited spontaneous beating (Figure 1B, Online Video I). We isolated SAN tissue and right atrial (RA) myocardium by laser capture micro-dissection (LCM) on unfixed, unstained cryosections from flash frozen *Hcn4*-GFP hearts harvested at E14.5, P4, and P14 (Figure 1C, Online Video II). The SAN is heterogeneous and includes non-PC cells such as fibroblasts, endothelial cells, and atrial cardiomyocytes. To optimize enrichment for PCs, we selected regions of interest for LCM within the SAN head (near the SAN artery) that contained purer populations of PCs (Online Figure I). Such regions within the SAN, as well as neighboring RA regions, were excised from 6 consecutive embryonic heart sections and pooled to generate total RNA. We repeated the LCM experiment for three different embryos for each time point to generate 18 independent RNA samples, reflecting 3 biological replicates for each tissue and time point (Online Table I). Each sample was processed separately for RNA-sequencing (RNA-seq) as described in the online methods section.

Differential expression analysis

Differential expression (DE) analysis of RNA-seq data between SAN and RA tissue samples revealed hundreds of DE genes at each time point (Online Table II). Known SAN-associated genes *Hcn4*, *Tbx3*, *Shox2*, *Tbx18*, and *Bmp4* were all enriched in the SAN tissue, while RA-associated genes *Nkx2-5*, *Nppa*, and *Gjal* were enriched in the RA samples (Online Figure I), demonstrating the fidelity of tissue isolation. Of note, the core cardiac transcription factors *Gata4*, *Mef2c* and *Tbx5*, were not differentially expressed between SAN and RA. We also found numerous genes enriched in the SAN tissue that had not been previously associated with PCs (Figure 2A, Online Table II). Gene Ontology terms (GO) associated with SAN-enriched genes included *Bmp* and *Wnt* signaling pathways at E14.5, and neuronal development and function at later time points (Figure 2A, Online Table III). Conversely, RA-enriched genes were associated with GO terms that included conduction, contractile apparatus, and cell junction formation (Figure 2B, Online Table III). While a core set of genes in each tissue type exhibited DE at all time points examined (Online Table IV), there was considerable change over time within the DE gene set, highlighting the dynamic nature of expression during SAN development. Hierarchical clustering of SAN and RA samples revealed that biological replicates clustered together, and that, as differentiation progressed, SAN samples were more similar to each other than they were to the RA samples (Online Figure II).

Network analysis

We employed weighted gene correlation network analysis (WGCNA) to partition the RA and SAN transcriptomes into modules exhibiting correlated gene expression (Online Figure III, Online Table V). Most time points of specific tissue were associated with at least one highly active module. Module 1 (M1) exhibited highest activity at E14.5, a critical period for SAN morphogenesis and PC differentiation (Figure 2C). M1 contained several previously identified SAN-enriched transcription factors, including *Tbx18*, *Shox2*, and *Isl1*, while *Tbx3* clustered with *Hcn4* and *Hcn1* in M7. Of the factors in M1, *Isl1* had the highest level of DE as well as high transcript abundance early in SAN development (Figure 2D).

Conditional selection of *Isl1* after second heart field differentiation

To test for a requirement of *Isl1* in the PC gene expression program, we crossed *Isl1^{loxp/loxp}; CAG-Cre/Esr1* with *Isl1^{loxp/loxp}; Hcn4-GFP* and injected intra-peritoneal tamoxifen at E10.5 (Figure 3A). This strategy generated a global deletion of *Isl1* after second heart field differentiation, which circumvented the early embryonic lethality associated with *Isl1* loss of function. *Cre⁺;Hcn4-GFP⁺* embryos were recovered at Mendelian ratios at E12.5, indicating that loss of *Isl1* after second heart field differentiation did not lead to rapid embryonic demise. SAN *Hcn4-GFP* expression was reduced but readily detectable in *Cre⁺* embryos (Figure 3B).

We then performed LCM on *Cre⁺* and *Cre⁻* embryonic SAN at E12.5. Each sample was pooled from approximately 9 SAN sections per embryo, and we used 7 different embryos (3 for *Cre⁺* group and 4 for *Cre⁻* group, Figure 3B). Quantitative PCR performed on amplified cDNA prior to RNA-Seq library preparation could not detect *Isl1* transcript in the samples from *Cre⁺* embryos, a finding confirmed by the absence of RNA-Seq reads mapped to the floxed portion of *Isl1* (Online Figure IV).

SAN transcriptome in the absence of *Isl1*

590 genes exhibited DE between *Cre⁺* and *Cre⁻* RNA samples, of which 65% were downregulated in SAN tissue lacking *Isl1* (Figure 3C, Online Table VI). Among the genes enriched in SAN tissue vs. RA at E14.5, 18% were downregulated after deletion of *Isl1* (odds ratio (OR) = 14, $p=1.1 \times 10^{-88}$, compared to non-DE genes), indicating a positive role for *Isl1* in the PC-specific gene expression program. Of genes with established roles in SAN development and PC function, *Tbx3*, *Hcn4*, *Hcn1*, and *Cacna1g* were all significantly decreased after deletion of *Isl1*, while expression of other cardiac and SAN TFs including *Nkx2.5*, *Gata4*, *Mef2C*, *Tbx5*, and *Tbx18* were not significantly changed (Figure 3D). Conversely, 9% of RA-enriched genes (including *Nppa*, *Gja1*, *Gja5*, and *Scn5a*) were upregulated in SAN after loss of *Isl1* (OR = 10, $p=9.6 \times 10^{-35}$), suggesting a secondary role for *Isl1* in repressing a differentiation program associated with working myocardium.

Network and motif analysis on dysregulated genes

Assessment of individual network activity after loss of *Isl1* function showed that M7 (containing *Hcn4* and *Tbx3*), followed by M1 (containing *Tbx18*, *Shox2* and *Isl1*), were the most reduced in overall activity (Online Figure VI). Conversely, the only modules that exhibited increased activity after loss of *Isl1*, M3 and M9, were associated with increased activity in RA. To relate these global changes in expression to loss of *Isl1* function, we searched for *Isl1* binding sites within introns, untranslated regions, and 10 kb upstream of the transcriptional start sites of genes that were downregulated after loss of *Isl1*, and compared the frequency of occurrence of these sites to genes that were unaffected by *Isl1* deletion. This analysis showed highly significant enrichment ($p = 0.0003$) of *Isl1* binding sites among the genes downregulated after *Isl1* deletion, suggesting a role for *Isl1* as a direct transcriptional activator in the developing SAN (Figure 4A, Online Figure VI). Examples of putative *Isl1* binding sites in *Tbx3* and *Hcn4* regulatory regions are shown in Online Table VII. Because of the limiting number of pacemaker cells in each embryonic heart, it was not

possible to test these sites directly using chromatin immunoprecipitation. Conversely, we did not observe enrichment of *Isl1* binding sites near the genes upregulated after *Isl1* deletion, suggesting that *Isl1* may not function primarily as a direct transcriptional repressor of these genes, but may suppress the atrial gene expression program indirectly (Figure 4B, Online Figure V).

Sensitivity analysis

Because inadvertent contamination of a Cre⁺ SAN sample with non-PC myocytes would bias our analysis towards the observed effects, we assessed our SAN samples for the presence of outliers. We found that one of the three Cre⁺ samples consistently exhibited more dramatic changes in gene expression at more diverse loci than the other two samples, raising the possibility of either contamination by non-PC myocytes or simply biological variation. To insure the robustness of our findings, we repeated our differential expression analysis and motif analysis after excluding this outlier sample and observed no significant changes in our results (Online Table VII, Online Figure VI).

DISCUSSION

Here, we present a comprehensive transcriptional analysis of mammalian PCs by deep sequencing SAN tissue obtained with LCM. While PCs and RA myocytes share core transcriptional machinery, mature PCs have adopted a distinct transcriptional program, consistent with morphological and electrical phenotypes exhibited by PCs. Our dataset highlights dynamic changes in PC gene expression associated with differentiation and maturation, and reveals a central role of *Isl1* in establishing the PC gene program.

Establishment and utility of SAN-specific gene networks

Knowledge of the SAN transcriptome is a prerequisite to understanding the unique properties of this specialized cell type and its disruption in the setting of disease. In addition, the description of the major regulators and networks activated and repressed in the SAN provides a foundation for studies aimed at regulating SAN cell fate. Because of the difficulty of isolating pure PC RNA, there has been no dataset to use for comparison of putatively reprogrammed PCs with endogenous PCs. Because some non-PC cardiomyocytes can exhibit automaticity with PC-like action potentials,^{12, 13} and many SAN-associated genes such as *Hcn4* exhibit dynamic expression outside the SAN,¹⁴ it is ideal to have a characteristic transcriptome as a means to determine the degree of fidelity during reprogramming.¹⁵

Our SAN expression profile can provide such a benchmark for investigators attempting to derive PCs from non-PCs and will permit more precise characterization of putatively reprogrammed cells. Analysis of specific gene sets with discordant expression between *bona fide* PCs and reprogrammed PCs may lead to targeted refinements of current methods. In addition, by quantifying changes in SAN gene expression during development, our dataset may suggest ways to promote maturation of incompletely reprogrammed cells.

Role of *Isl1* in establishing the SAN gene network

Isl1 is required for second heart field development in mice¹⁶ and for SAN development in zebrafish.⁶ Although *Isl1* expression and function in mouse PCs has been described previously,^{7, 17} its transcriptional role in the SAN remains unknown. Our loss of function data demonstrated that SAN-enriched genes were strongly overrepresented among the genes downregulated after *Isl1* disruption, suggesting that *Isl1* is required to generate the SAN-specific gene expression program. Furthermore, we observed significant enrichment of *Isl1* binding sites within and around downregulated genes, providing strong evidence that *Isl1* is a direct transcriptional activator of gene expression in PCs.

We also observed upregulation of genes associated with RA myocardium in the SAN after deletion of *Isl1*, including *Nppa*, *Scn5a*, *Gja1*, and *Gja5*. However, we did not observe enrichment of *Isl1* binding sites near the upregulated genes, suggesting that *Isl1* functions indirectly to block the RA myocyte gene expression in the SAN. *Tbx3* is an established negative regulator of the atrial myocyte gene expression program⁴ and was found in our analysis to be highly downregulated after deletion of *Isl1*. One possibility is that upregulation of RA genes after *Isl1* deletion is mediated in part by downregulation of *Tbx3* (Figure 4C). This model situates *Isl1* as a key transcriptional activator in PCs with a major role in establishing the SAN-specific gene expression program. As the scope of the present study is limited to expression analysis, further work will be required to delineate the functional and developmental roles of *Isl1* in sinoatrial node, and to validate putative direct transcriptional targets. In addition, the potential of *Isl1* to augment PC derivation or reprogramming has yet to be fully explored. Our analysis suggests that multifactor reprogramming using *Isl1* in combination with other cardiac and/or SAN transcription factors may be a fruitful approach.

Acknowledgments

We thank the Gladstone Genomics Core, the UCSF Center for Advanced Technology, and the Gladstone Bioinformatics Core for assistance with RNA library preparation, RNA sequencing, and initial sequence analysis, respectively. LCM was performed at the UCSF Laboratory for Cell Analysis.

SOURCES OF FUNDING

The authors were funded by the NIH/NHLBI (K08 HL101989 to V.V.; K08 HL093861, DP2 HL123228, and U01 HL107440-03 to R.C.D.; R01 HL057181, P01 HL089707 U01 HL100406, and U01 HL098179 to D.S.), the AHA (14BGIA20490269 to V.V.), the Younger Family Foundation, the Roddenberry Foundation, and the California Institute for Regenerative Medicine (to D.S.).

Nonstandard Abbreviations and Acronyms

SAN	sinoatrial node
RA	right atrium
PC	pacemaker cell
LCM	laser capture micro-dissection
GFP	green fluorescent protein

M	gene expression module
Cre	Cre Recombinase
DE	Differential expression
GO	Gene ontology

References

1. Qian L, Srivastava D. Direct cardiac reprogramming: from developmental biology to cardiac regeneration. *Circ Res.* 2013; 113:915–921. [PubMed: 24030021]
2. Takahashi K. Cellular reprogramming. *Cold Spring Harb Perspect Biol.* 2014;6.
3. Wiese C, Grieskamp T, Airik R, Mommersteeg MT, Gardiwal A, de Gier-de Vries C, Schuster-Gossler K, Moorman AF, Kispert A, Christoffels VM. Formation of the sinus node head and differentiation of sinus node myocardium are independently regulated by Tbx18 and Tbx3. *Circ Res.* 2009; 104:388–397. [PubMed: 19096026]
4. Hoogaars WM, Engel A, Brons JF, Verkerk AO, de Lange FJ, Wong LY, Bakker ML, Clout DE, Wakker V, Barnett P, Ravesloot JH, Moorman AF, Verheijck EE, Christoffels VM. Tbx3 controls the sinoatrial node gene program and imposes pacemaker function on the atria. *Genes Dev.* 2007; 21:1098–1112. [PubMed: 17473172]
5. Blaschke RJ, Hahurij ND, Kuijper S, Just S, Wisse LJ, Deissler K, Maxelon T, Anastassiadis K, Spitzer J, Hardt SE, Scholer H, Feitsma H, Rottbauer W, Blum M, Meijlink F, Rappold G, Gittenberger-de Groot AC. Targeted mutation reveals essential functions of the homeodomain transcription factor Shox2 in sinoatrial and pacemaking development. *Circulation.* 2007; 115:1830–1838. [PubMed: 17372176]
6. Tessadori F, van Weerd JH, Burkhard SB, Verkerk AO, de Pater E, Boukens BJ, Vink A, Christoffels VM, Bakkers J. Identification and functional characterization of cardiac pacemaker cells in zebrafish. *PLoS ONE.* 2012; 7:e47644. [PubMed: 23077655]
7. Weinberger F, Mehrkens D, Friedrich FW, Stubbendorff M, Hua X, Muller JC, Schrepfer S, Evans SM, Carrier L, Eschenhagen T. Localization of Islet-1-positive cells in the healthy and infarcted adult murine heart. *Circ Res.* 2012; 110:1303–1310. [PubMed: 22427341]
8. Bakker ML, Boink GJ, Boukens BJ, Verkerk AO, van den Boogaard M, den Haan AD, Hoogaars WM, Buermans HP, de Bakker JM, Seppen J, Tan HL, Moorman AF, t Hoen PA, Christoffels VM. T-box transcription factor TBX3 reprogrammes mature cardiac myocytes into pacemaker-like cells. *Cardiovasc Res.* 2012; 94:439–449. [PubMed: 22419669]
9. Kapoor N, Liang W, Marban E, Cho HC. Direct conversion of quiescent cardiomyocytes to pacemaker cells by expression of Tbx18. *Nat Biotechnol.* 2013; 31:54–62. [PubMed: 23242162]
10. Hu YF, Dawkins JF, Cho HC, Marban E, Cingolani E. Biological pacemaker created by minimally invasive somatic reprogramming in pigs with complete heart block. *Sci Transl Med.* 2014; 6:245ra294.
11. Nam YJ, Lubczyk C, Bhakta M, Zang T, Fernandez-Perez A, McAnally J, Bassel-Duby R, Olson EN, Munshi NV. Induction of diverse cardiac cell types by reprogramming fibroblasts with cardiac transcription factors. *Development.* 2014; 141:4267–4278. [PubMed: 25344074]
12. Yasui K, Liu W, Opthof T, Kada K, Lee JK, Kamiya K, Kodama I. I(f) current and spontaneous activity in mouse embryonic ventricular myocytes. *Circ Res.* 2001; 88:536–542. [PubMed: 11249878]
13. Zhang Q, Timofeyev V, Qiu H, Lu L, Li N, Singapuri A, Torado CL, Shin HS, Chiamvimonvat N. Expression and roles of Cav1.3 (alpha1D) L-type Ca(2)+ channel in atrioventricular node automaticity. *J Mol Cell Cardiol.* 2011; 50:194–202. [PubMed: 20951705]
14. Liang X, Wang G, Lin L, Lowe J, Zhang Q, Bu L, Chen Y, Chen J, Sun Y, Evans SM. HCN4 dynamically marks the first heart field and conduction system precursors. *Circ Res.* 2013; 113:399–407. [PubMed: 23743334]

15. Morris SA, Cahan P, Li H, Zhao AM, San Roman AK, Shivdasani RA, Collins JJ, Daley GQ. Dissecting engineered cell types and enhancing cell fate conversion via CellNet. *Cell*. 2014; 158:889–902. [PubMed: 25126792]
16. Cai CL, Liang X, Shi Y, Chu PH, Pfaff SL, Chen J, Evans S. Isl1 identifies a cardiac progenitor population that proliferates prior to differentiation and contributes a majority of cells to the heart. *Dev Cell*. 2003; 5:877–889. [PubMed: 14667410]
17. Hoffmann S, Berger IM, Glaser A, Bacon C, Li L, Gretz N, Steinbeisser H, Rottbauer W, Just S, Rappold G. Islet1 is a direct transcriptional target of the homeodomain transcription factor Shox2 and rescues the Shox2-mediated bradycardia. *Basic Res Cardiol*. 2013; 108:339. [PubMed: 23455426]

Novelty and Significance

What Is Known?

- Cardiac pacemaker cells (PCs) in the sinoatrial node (SAN) have a distinct gene expression program that underlies their unique functional properties, but are difficult to isolate in sufficient quantity and with adequate purity required for expression profiling.
- Non-PC myocytes can be reprogrammed to exhibit PC-like behavior using SAN transcription factors, with varying efficiency and uncertain fidelity.

What New Information Does This Article Contribute?

- Pure SAN tissue was isolated at mid-development, the perinatal period, and after maturation for comprehensive expression profiling using RNA sequencing.
- Differential expression analysis of SAN tissue and right atrial tissue uncovered numerous SAN-enriched genes not previously associated with PCs.
- RNA sequencing of SAN tissue in the absence of the transcription factor *Islet-1* (*Isl1*) showed that *Isl1* plays an important role in establishing the PC gene expression program during heart development.

The regeneration of sinoatrial node (SAN) or the creation of biological pacemakers using cellular reprogramming are promising new approaches to the treatment of sinus node disease (SND). Further development of these therapies will require a detailed understanding of transcriptional networks in specialized cardiac pacemaker cells (PC). However, these cells are difficult to characterize because they are few in number, they lack of specific molecular markers, and they are interspersed among non-PC cells. In this study, we used laser capture microdissection to isolate purer populations of PCs from embryonic, perinatal, and postnatal SAN for RNA sequencing. Analysis of RNA sequencing data uncovered numerous genes expressed in SAN that were not previously associated with PCs. Based on high differential expression, high absolute expression, and a weighted gene correlation network analysis, the transcription factor *Isl1* was predicted to regulate PC-specific gene expression. RNA-Seq on SAN tissue lacking *Isl1* confirmed this prediction and established *Isl1* as an important transcriptional regulator within the developing SAN. The results of this study could form the basis of further mechanistic investigations into the gene regulatory networks active in the SAN and future translational work on SND.

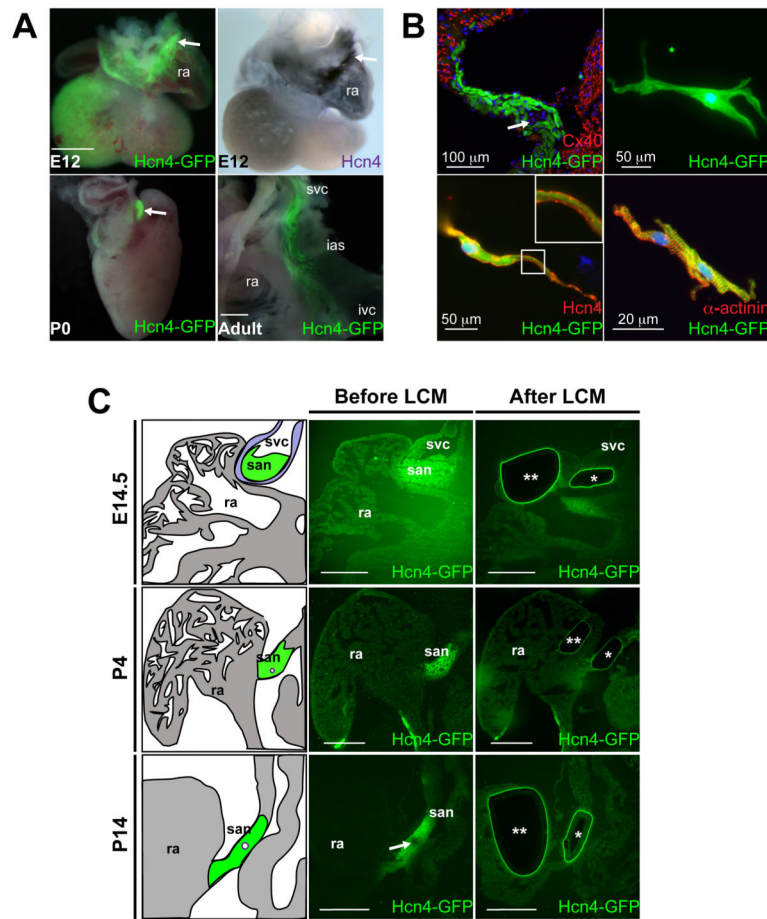


Figure 1. Laser Capture Micro-Dissection of Sinoatrial Node Pacemaker Cells from *Hcn4*-GFP BAC Transgenic

(A) Whole-mount images of embryonic day (E) 12.5 hearts (top, left), post-natal day 0 (P0, bottom, left), and adult right atrium (bottom right) showed expression of *Hcn4*-GFP, compared to *in-situ* hybridization for *Hcn4* (top, right). Arrows denote sinoatrial node (SAN). At the adult stage, GFP⁺ cells were present in the mature SAN, located in the intercaval groove between the inter-atrial septum (ias) and right atrium (ra). (B) Immunohistochemistry on adult SAN from *Hcn4*-GFP hearts showing complementary expression of GFP and Connexin-40 (Cx40) (arrow denotes SAN artery). Isolated *Hcn4*-GFP⁺ cells (top, right), were Hcn4⁺ by immunocytochemistry (bottom, left – high magnification inset shows Hcn4 immunostaining at cell membrane) and were positive for the myocyte marker α -actinin (bottom, right). (C) Unfixed, unstained sections from *Hcn4*-GFP hearts were used for laser capture microdissection (LCM) of SAN and RA at time points indicated. Schematic depictions of the SAN and RA are shown for corresponding sections before or after LCM. Arrows denote SAN artery; ‘*’ denotes the excised SAN region and ‘**’ denotes excised right atrial tissue; svc, superior vena cava; ivc, inferior vena cava. Scalebars = 200 μ M unless otherwise indicated.

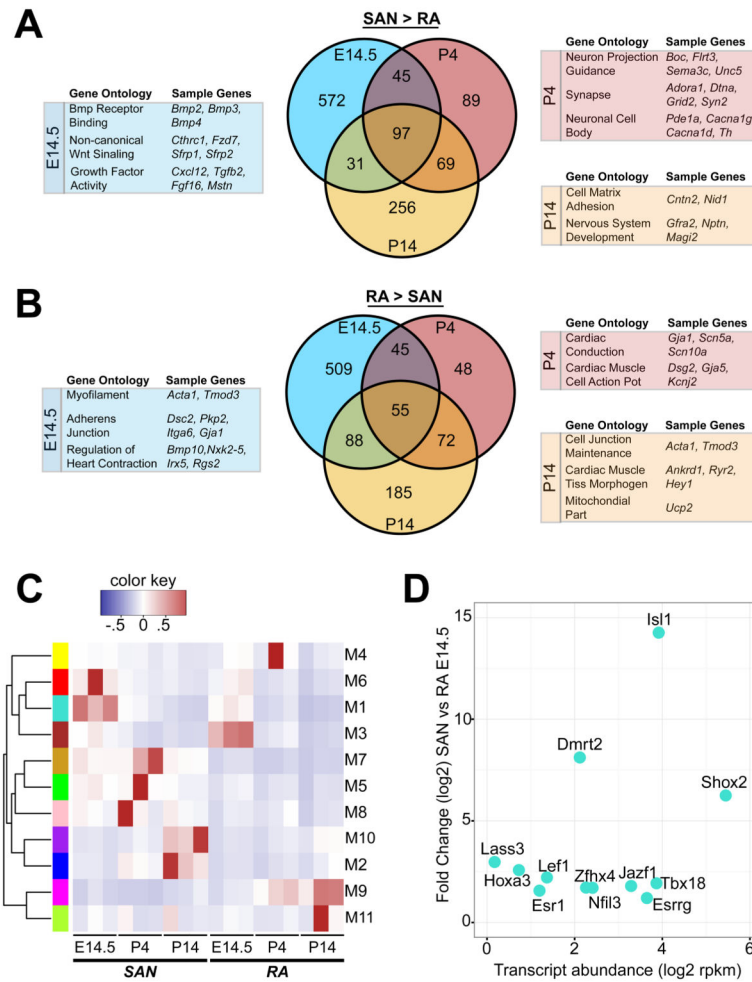


Figure 2. Comparative Expression Analysis of SAN and RA

(A) Venn diagram showing overlap of SAN-enriched genes at E14.5, P4, and P14 using a false discovery rate cutoff of 0.05. Selected enriched gene ontology terms with example genes are shown for each time point. (B) Similar Venn diagram as (A), but for RA-enriched genes. (C) Weighted gene correlation network analysis (WGCNA) identified 11 highly correlated modules within SAN/RA data set. Module eigengene activity was computed for each module for each of the 18 SAN/RA expression time points. Color key indicates activity scale. (D) Expression of SAN-enriched transcription factors within Module 1 at E14.5. Transcript levels are shown on the X-axis and differential expression (SAN vs RA) on the Y-axis. Abbreviations: SAN, sinoatrial node; RA, right atrium.

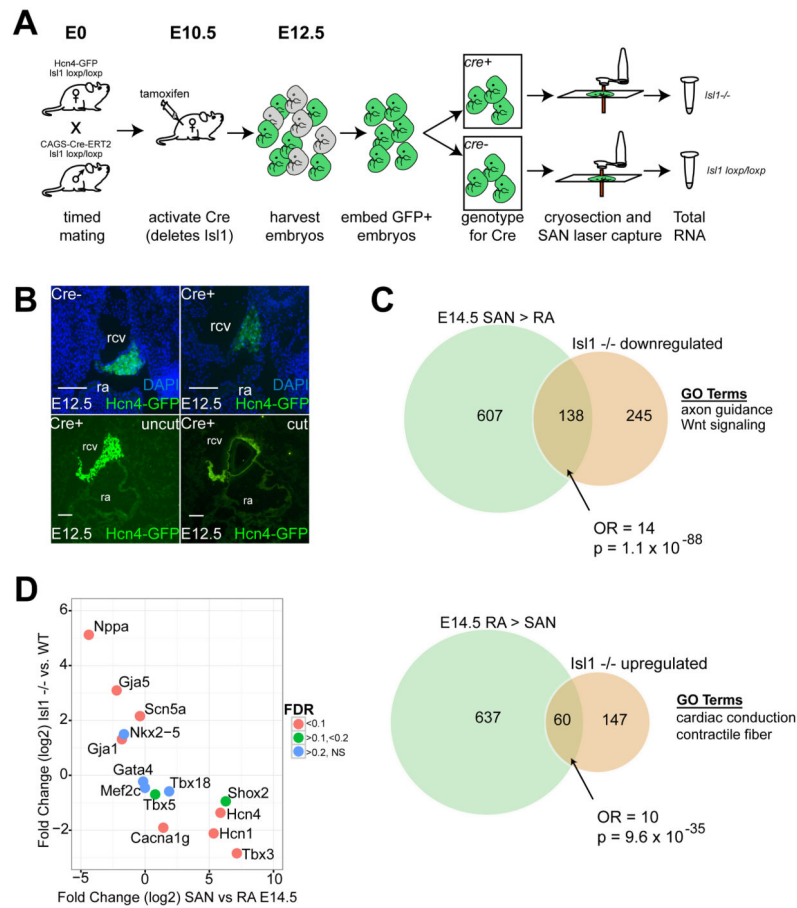


Figure 3. SAN Transcriptome After *Isl1* Deletion

(A) Strategy to obtain RNA from SAN tissue lacking *Isl1*. (B). Top row: Immunohistochemistry of E12.5 SAN in *Cre*⁻ embryos, with intact *Isl1* expression (left) in comparison to *Cre*⁺ embryos (right) which lack *Isl1*. DAPI staining indicates nuclei. Bottom row: adjacent sections from *Cre*⁺ E12.5 SAN lacking *Isl1*. Left, uncut, and right, after laser capture microdissection. Scalebars = 100 μ m (C) Venn diagrams showing statistically significant overlap of genes enriched in SAN (top) or RA (bottom) at E14.5 with genes that were downregulated (top) or upregulated (bottom) after *Isl1* deletion. (D) Scatterplot showing that *Isl1* results in downregulation of SAN-enriched genes and upregulation of RA-enriched genes. Abbreviations: rcv, right cardinal vein; ra, right atrium; NS, non-significant.

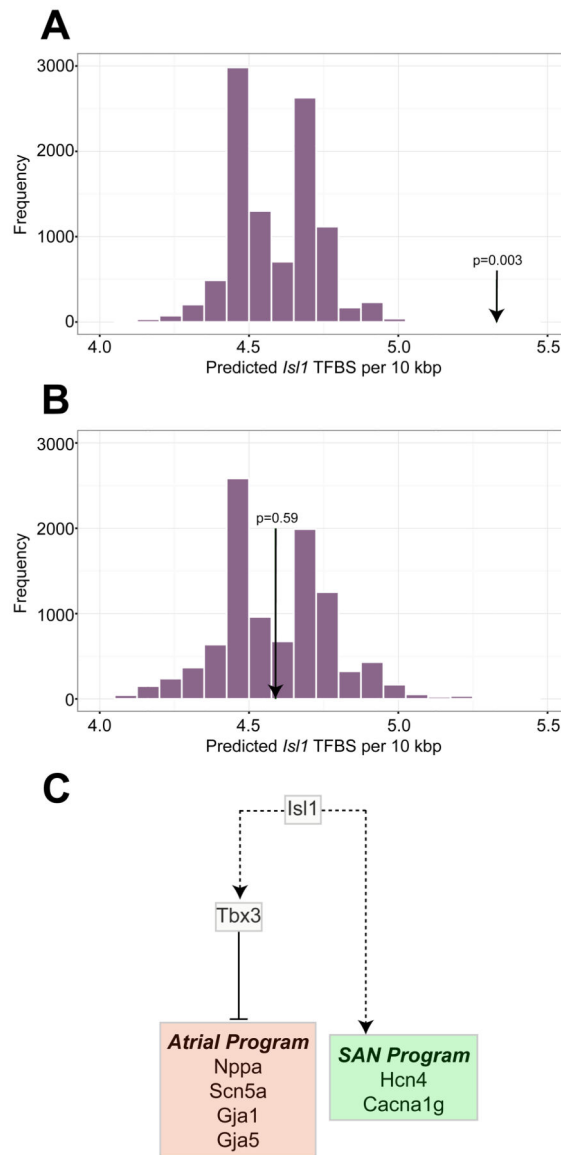


Figure 4. Inferring Isl1 Function in Cardiac Pacemaker Cells

(A) For motif analysis on *Isl1* binding sites, regions up to 10kb upstream of the transcriptional start site, introns, and untranslated regions for genes downregulated after *Isl1* deletion were included in the query set. A null set was defined as genes that were not differentially expressed. The histogram shows a distribution of medians of 10,000 samples drawn from the null set by bootstrap sampling. The arrow denotes the observed frequency of *Isl1* binding sites among genes downregulated after *Isl1* deletion. (B) Similar motif analysis to (A), where the arrow denotes the observed frequency of *Isl1* binding sites at genes upregulated after loss of *Isl1*. (C) A model for *Isl1* transcriptional activity in the SAN. A solid line indicates a direct transcriptional relation; dashed lines indicate hierarchical relationships based on expression analysis only (may be direct or indirect).